Novel Graphical Approach to Analyze the Stability of TCP/AQM Networks

GE Long[1, 2] FANG Bin[1] SUN Jin-Sheng[1] WANG Zhi-Quan[1]

Abstract In order to set controller parameters correctly, a graphical stability analysis approach for active queue management (AQM) is proposed. The model of TCP/AQM is converted into a second-order system with time delay. The stability of the closed-loop AQM system is described in terms of characteristic quasi-polynomial. New necessary and sufficient stability criterion is deduced based on the inverse Nyquist curve and the negative frequency characteristic line. The relations between stabilizing boundary of proportional gain in PID controller and network parameters are investigated. Different stabilizing regions are compared to show the less conservatism of our approach, and simulation experiments implemented by both Matlab and Network Simulator validate our analysis. The specialty of the proposed approach lies in the lower complexity of the calculation procedure and intuition in the complex plane.

Key words Network congestion control, active queue management, stability analysis, time-delay, quasi-polynomials

DOI 10.3724/SP.J.1004.2010.00314

It is well known that the transmission control protocol (TCP) has a mechanism to adjust the packet sending rate by probing the congestion. However, the end-to-end TCP congestion control is not sufficient to provide satisfactory performance in terms of overall quality of service (QoS). Active queue management (AQM) plays a key role in the intermediate router to complement the endpoint congestion avoidance mechanism, which attempts to estimate the congestion and signal the incipient congestion by marking/dropping packets before the buffer is full.

Random early detection (RED)[1] is the first well known AQM algorithm, which aims to achieve fairness among multi-sources and control the queue length to the desired range. From the viewpoint of control theory, the AQM scheme works as a feedback control law. It enables us to use the control principles to analyze and design AQM controllers in the network environment. This study is based on the use of a dynamic model of TCP/AQM[2]. The Network Simulator (NS) simulation demonstrates that this model accurately captures the TCP′s dynamic behavior. In [3], this nonlinear model was linearized at an operating point to address the feedback control nature. Proportional (P) and proportional-integral (PI) AQM controllers were introduced by comparison to RED. In [4], structural nonlinear component of RED was considered, and the describing function approach was applied to obtain a stability criterion for RED. In [5], an improved PI controller was proposed, which adaptively adjusted the controller parameters based on network parameters estimation.

In order to stabilize the network traffic system and achieve the desired QoS, [6−11] paid much attention to the setting of controller parameters. In [6], pole assignment approach was adopted to obtain the higher utilization and congestion avoidance. In [7], a stabilizing optimal gain for proportional-integral-derivative (PID) controller was constructed based on state space model. In [8−9], PID controllers were designed analytically using H_∞ optimal control theory. In [10−11], PID controllers were designed based on the integral of time-weighted absolute error (ITAE) and integral of absolute error (IAE) performance, respectively.

It is interesting to note that even though most of these setting techniques provide effective results[6−11], the stabilizing region of controller parameters for TCP/AQM model with time delay remains unknown. The fact motivates this paper. Our objective is to characterize the stabilizing region of PID controller to guarantee parameters in which could stabilize the second-order system with time delay. In earlier work, when the AQM controller is of P type, in the case of delay-free marking, the system′s equilibrium point is stable for all proportional gains. In a more realistic case of delayed feedback, there exists a boundary for proportional gain to guarantee the closed-loop AQM system stability[12]. When the AQM controller is of PI type, the stabilizing boundary of proportional gain has been given by using a parameter space approach[13].

In this paper, when the AQM controller is of PID type, a novel graphical stability criterion for closed-loop AQM system is proposed, which is based on observing the inverse Nyquist curve and the negative frequency characteristic line in complex plane. The necessary and sufficient stability criterion is employed to investigate the stabilizing boundary of proportional gain directly, and its relations with the network parameters are illuminated. The stabilizing region of AQM controller in PID type is given in three-dimensional graph. At last, comparisons and simulations are conducted to prove our criterion.

1 TCP/AQM model

1.1 Simplified dynamics

A dynamic model of TCP behavior is developed based on fluid-flow and stochastic differential equation[2], which is difficult to deal with due to its complexity. The following version ignores the TCP timeout mechanism[3].

$$\begin{cases} \dot{W}(t) = \dfrac{1}{R(t)} - \dfrac{W(t)W(t-R(t))}{2R(t-R(t))}p(t-R(t)) \\ \dot{q}(t) = \dfrac{N(t)}{R(t)}W(t) - C(t) \end{cases} \tag{1}$$

where $\dot{W}(t)$ and $\dot{q}(t)$ denote the time-derivatives of $W(t)$ and $q(t)$, respectively. $W(t)$ denotes the TCP window size. $q(t)$ denotes the queue length in the router. $p(t)$ denotes the probability of packet marking/dropping ($p(t) \in [0, 1]$). $R(t)$ denotes the round-trip time, where $R(t) = q(t)/C(t) + T_p$.

Manuscript received October 29, 2008; accepted June 22, 2009
Supported by National Natural Science Foundation of China (60974129, 70931002), Natural Science Foundation of Jiangsu Province (BK2008188, BK2009388), and Science Foundation of Nanjing University of Science and Technology (AB41972)
1. School of Automation, Nanjing University of Science and Technology, Nanjing 210094, P. R. China 2. Changshu Science and Technology Bureau, Changshu 215500, P. R. China

$C(t)$ denotes the link capacity. T_p denotes the propagation delay. $N(t)$ denotes the load factor (number of TCP sessions).

Taking (W, q) as state variable and p as input, we define the operating point (W_0, q_0, p_0) as $\dot{W}(t) = 0, \dot{q}(t) = 0$. That is, $W_0 = \dfrac{R_0 C}{N}$, $p_0 = \dfrac{2}{W_0^2}$. Using linearization techniques near the operating point of the nonlinear differential equation (1), we obtain a linear differential equation of the TCP/AQM model[3].

$$\begin{cases} \delta\dot{W}(t) = -\dfrac{N}{R_0^2 C}(\delta W(t) + \delta W(t - R_0)) - \\ \qquad \dfrac{1}{R_0^2 C}(\delta q(t) - \delta q(t - R_0)) - \dfrac{R_0 C^2}{2N^2}\delta p(t - R_0) \\ \delta\dot{q}(t) = \dfrac{N}{R_0}\delta W(t) - \dfrac{1}{R_0}\delta q(t) \end{cases} \tag{2}$$

where $\delta W = W - W_0, \delta q = q - q_0, \delta p = p - p_0$.

For typical network conditions[3] $\dfrac{N}{R_0^2 C} = \dfrac{1}{W_0 R_0} \ll \dfrac{1}{R_0}$, we just consider the following dynamics.

$$\begin{cases} \delta\dot{W}(t) = -\dfrac{2N}{R_0^2 C}\delta W(t) - \dfrac{R_0 C^2}{2N^2}\delta p(t - R_0) \\ \delta\dot{q}(t) = \dfrac{N}{R_0}\delta W(t) - \dfrac{1}{R_0}\delta q(t) \end{cases} \tag{3}$$

Performing Laplace transform on (3), we have

$$G_{\mathrm{TCP}}(s) = \frac{\dfrac{R_0 C^2}{2N^2}}{s + \dfrac{2N}{R_0^2 C}} \mathrm{e}^{-sR_0} \tag{4}$$

$$G_{\mathrm{queue}}(s) = \frac{\dfrac{N}{R_0}}{s + \dfrac{1}{R_0}} \tag{5}$$

where $G_{\mathrm{TCP}}(s)$ denotes the TCP′s dynamic, and $G_{\mathrm{queue}}(s)$ denotes the queue′s dynamic. The block diagram of the AQM system presents as Fig. 1.

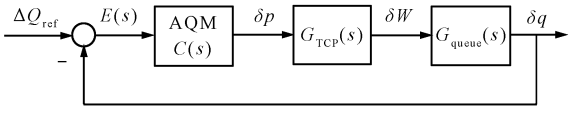

Fig. 1 Block diagram of the AQM system

1.2 Characteristic quasi-polynomial

Consider the closed-loop AQM system with $G(s)$ being the transcendental function of the plant and $C(s)$ being the transfer function of the controller.

$$G(s) = G_{\mathrm{TCP}}(s)G_{\mathrm{queue}}(s) = \frac{P(s)}{Q(s)}\mathrm{e}^{-\tau s} \tag{6}$$

where $P(s) = k, Q(s) = (s + T_1)(s + T_2), k = \dfrac{C^2}{2N}, T_1 = \dfrac{2N}{R_0^2 C}, T_2 = \dfrac{1}{R_0}, \tau = R_0$. As the network parameters $\{N, C, R_0\}$ are positive, the model parameters $\{k, T_1, T_2, \tau\}$ are positive.

$$C(s) = k_{\mathrm{p}} + \frac{k_{\mathrm{i}}}{s} + k_{\mathrm{d}} s \tag{7}$$

The closed-loop AQM system is a second-order system with time delay, whose characteristic equation is

$$1 + C(s)G(s) = 0 \tag{8}$$

and characteristic quasi-polynomial is

$$\Delta(s) = s(s + T_1)(s + T_2) + k(k_{\mathrm{i}} + k_{\mathrm{p}} s + k_{\mathrm{d}} s^2)\mathrm{e}^{-\tau s} \tag{9}$$

Multiplying both sides of (9) by $\mathrm{e}^{\tau s}$ yields

$$\Delta^*(s) = s(s + T_1)(s + T_2)\mathrm{e}^{\tau s} + k(k_{\mathrm{i}} + k_{\mathrm{p}} s + k_{\mathrm{d}} s^2) \tag{10}$$

As $\mathrm{e}^{\tau s}$ does not have any finite zeros, the zeros of $\Delta(s)$ are identical to those of $\Delta^*(s)$. The characteristic quasi-polynomial $\Delta(s)$ of the closed-loop AQM system is stable if and only if the zeros of $\Delta^*(s)$ are in open left hand plane (LHP). Then, $\Delta^*(s)$ is defined as Hurwitz or stable.

The problem of stability verification for linear system with time delay involves finding the location of the roots of transcendental functions. The classical method is the Nyquist criterion. However, for the analytical characterization of the stabilizing gain, we have to deal with non-linear inequalities.

To determine the region of controller parameters for the closed-loop AQM system to be stable, a novel graphical stability criterion will be deduced in next section.

2 Graphical stability criterion

2.1 Extended Hermite-Biehler theorem

Consider a class of linear system with time delay, which has characteristic function described by a quasi-polynomial with the form

$$\delta(s) = d(s) + \sum_{i=1}^{m} \mathrm{e}^{-sT_i} n_i(s) \tag{11}$$

where $d(s), n_i(s)$ for $i = 1, \cdots, m$ are polynomials with real coefficients, and $0 < T_1 < T_2 < \cdots < T_m$.

Substituting $s = \mathrm{j}\omega$ into (11), we have

$$\delta(\mathrm{j}\omega) = \delta_r(\omega) + \mathrm{j}\delta_i(\omega) \tag{12}$$

where $\delta_r(\omega)$ and $\delta_i(\omega)$ represent the real and imaginary parts of the transcendental function associated with quasi-polynomial (11), respectively. The Hermite-Biehler theorem is extended as follows.

We make the following assumptions.

Assumption 1. $\mathrm{Deg}[d(s)] = n$, $\mathrm{Deg}[n_i(s)] < n$ for $i = 1, \cdots, m$.

Assumption 2. $d(s)$ and $n_i(s)$ for $i = 1, \cdots, m$ are coprime polynomials.

Lemma 1[14]**.** Consider quasi-polynomial (11). Under Assumption 1, $\delta(s)$ has all zeros in the open left half plane if and only if

1) $\delta_r(\omega)$ and $\delta_i(\omega)$ have only real roots and these roots interlace;

2) $\delta_i'(\omega_0)\delta_r(\omega_0) - \delta_i(\omega_0)\delta_r'(\omega_0) > 0$ for some ω_0 in $(-\infty, +\infty)$, where $\delta_r'(\omega)$ and $\delta_i'(\omega)$ denote the first derivatives with respect to ω of $\delta_r(\omega)$ and $\delta_i(\omega)$, respectively.

Remark 1. Condition 2) of Lemma 1 depicts the characteristic of $\delta(s)$ in complex plane. Phase angle of $\delta(\mathrm{j}\omega)$

increases with ω monotonically. A crucial step to use Lemma 1 to check stability is to ensure that $\delta_r(\omega)$ and $\delta_i(\omega)$ have only real roots. This condition is inconvenient to use. So, we have Lemma 2.

Lemma 2[15]**.** Consider real transcendental functions $\delta_r(\omega)$ and $\delta_i(\omega)$ in (12). Let M and N denote the highest powers of s and e^s of $\delta(s)$ in (11), respectively. Let η be an appropriate constant such that the coefficients of terms of highest degree in $\delta_r(\omega)$ and $\delta_i(\omega)$ do not vanish at $\omega = \eta$. For the equations $\delta_r(\omega) = 0$ or $\delta_i(\omega) = 0$ to have only real roots, it is necessary and sufficient that in the intervals

$$[-2L\pi + \eta, 2L\pi + \eta],\ L = 1, 2, 3, \cdots$$

$\delta_r(\omega)$ and $\delta_i(\omega)$ have exactly $4LN + M$ real roots starting with sufficiently large L.

Lemma 3[14]**.** Consider quasi-polynomial (11). Under Assumptions 1 and 2, there exists $\omega_0 \in (0, +\infty)$ such that $\delta_r(\omega)$ and $\delta_i(\omega)$ in (12) have only simple real roots and these roots interlace for $\omega > \omega_0$.

Remark 2. Lemma 3 illuminates that for $\omega > \omega_0$, where ω_0 is sufficiently large, under Assumptions 1 and 2, roots of $\delta(s)$ in (11) interlace, whether it is stable or not.

2.2 Stability criterion based on inverse Nyquist curve

We rewrite $\Delta^*(s)$ in (10) as

$$\delta(s) = sQ(s)\mathrm{e}^{\tau s} + (k_\mathrm{i} + k_\mathrm{p}s + k_\mathrm{d}s^2)P(s) = 0 \tag{13}$$

Substituting $z = \tau s$ into (13), we have

$$\delta(z) = zQ_1(z)\mathrm{e}^z + (k_\mathrm{i} + k_\mathrm{p}\tau^{-1}z + k_\mathrm{d}\tau^{-2}z^2)P_1(z) = 0 \tag{14}$$

where $Q_1(z) = \frac{1}{\tau}Q(\frac{z}{\tau})$ and $P_1(z) = P(\frac{z}{\tau})$.

Substituting $z = \mathrm{j}\omega_z$ into (14), we have

$$\delta(\mathrm{j}\omega_z) = \delta_r(\omega_z) + \mathrm{j}\delta_i(\omega_z) \tag{15}$$

Lemma 4. Consider quasi-polynomial (14). For $\delta(z)$ to be stable, it is necessary and sufficient that in the intervals

$$\omega_z \in [-2L\pi + \frac{\pi}{4}, 2L\pi + \frac{\pi}{4}],\quad L = 1, 2, 3, \cdots$$

$\delta_r(\omega_z)$ and $\delta_i(\omega_z)$ have exactly $4L + 3$ real roots and these roots interlace, with sufficiently large L.

Proof. Consider the reciprocal of $G(s)$ in (6),

$$\bar{G}(s) = \frac{1}{G(s)} = \frac{Q(s)}{P(s)}\mathrm{e}^{\tau s} \tag{16}$$

Substituting $s = \mathrm{j}\omega$ into (16), we have

$$\bar{G}(\mathrm{j}\omega) = \frac{1}{G(\mathrm{j}\omega)} = \frac{Q(\mathrm{j}\omega)}{P(\mathrm{j}\omega)}\mathrm{e}^{\mathrm{j}\tau\omega} = |\bar{G}(\mathrm{j}\omega)|\mathrm{e}^{\mathrm{j}\varphi(\omega)} \tag{17}$$

where $|\bar{G}(\mathrm{j}\omega)| = \dfrac{|Q(\mathrm{j}\omega)|}{|P(\mathrm{j}\omega)|}$ and $\varphi(\omega) = \angle Q(\mathrm{j}\omega) - \angle P(\mathrm{j}\omega) + \tau\omega$.

From (6), we have $P(\mathrm{j}\omega) = k$ and $Q(\mathrm{j}\omega) = (\mathrm{j}\omega + T_1)(\mathrm{j}\omega + T_2)$. It follows that $|P(\mathrm{j}\omega)| = k$ and $\angle P(\mathrm{j}\omega) = 0$ are constants. $|Q(\mathrm{j}\omega)|$ increases monotonically, and $\angle Q(\mathrm{j}\omega)$ seems to be a constant for $\omega > \omega_0$, with sufficiently large ω_0. As τ is positive, $\tau\omega$ increases linearly with ω. So, there exists a sufficiently large ω_0 such that $|\bar{G}(\mathrm{j}\omega)|$ and $\varphi(\omega)$ increase monotonically with ω for $\omega > \omega_0$. It means that the Nyquist curve of $\bar{G}(\mathrm{j}\omega)$ is a helix encircling the origin anticlockwise for $\omega > \omega_0$. It satisfies the phase angle condition 2) in Lemma 1.

$\delta(z)$ in (14) satisfies Assumptions 1 and 2. According to Lemma 3, there exists $\omega_0 \in (0, +\infty)$ such that $\delta_r(\omega_z)$ and $\delta_i(\omega_z)$ have only simple real roots and these roots interlace for $\omega > \omega_0$ ($\omega_z > \omega_{z0}$).

Then, we find a sufficiently large ω_0 such that two conditions above are satisfied at the same time. According to Lemma 1, for $\delta(z)$ to be stable, it is necessary and sufficient that $\delta_r(\omega_z)$ and $\delta_i(\omega_z)$ have only real roots and these roots interlace for $\omega < \omega_0$.

For $\delta(z)$ in (14), from Lemma 2, we have $M = 3, N = 1, \eta = \pi/4$. The coefficients of terms of highest degree in $\delta_r(\omega)$ and $\delta_i(\omega)$ do not vanish at $\omega = \pi/(4\tau)$ ($\omega_z = \pi/4$). For $\delta_r(\omega_z)$ and $\delta_i(\omega_z)$ to have only real roots, it is necessary and sufficient that in the intervals

$$\omega_z \in [-2L\pi + \frac{\pi}{4}, 2L\pi + \frac{\pi}{4}],\quad L = 1, 2, 3, \cdots$$

$\delta_r(\omega_z)$ and $\delta_i(\omega_z)$ have exactly $4L + 3$ real roots with sufficiently large L, where $2L\pi + \pi/4 > \omega_0$. □

Definition 1. The inverse Nyquist curve (INC) of plant $G(\mathrm{j}\omega)$ is defined as the Nyquist curve of $\bar{G}(\mathrm{j}\omega)$, where $\bar{G}(\mathrm{j}\omega) = \dfrac{1}{G(\mathrm{j}\omega)}$.

Definition 2. The negative frequency characteristic line (NFCL) of controller $C(\mathrm{j}\omega)$ is defined as $\mathrm{Re}[-C(\mathrm{j}\omega)] = -k_\mathrm{p}$, where $C(\mathrm{j}\omega) = k_\mathrm{p} + \dfrac{k_\mathrm{i}}{\mathrm{j}\omega} + k_\mathrm{d}\mathrm{j}\omega$.

Theorem 1. Plot the INC of AQM plant in (6) and the NFCL of PID controller in (7), for $\omega \in [0, (2L\pi + \pi/4)/\tau]$. For the characteristic quasi-polynomial of the closed-loop AQM system to be stable, it is necessary that the two curves have exactly M_0 intersections, where

$$M_0 = 2L + 1 \tag{18}$$

Proof. Substituting $s = \mathrm{j}\omega$ into (7) and (8), we have

$$-C(\mathrm{j}\omega) = -k_\mathrm{p} + \mathrm{j}(\frac{k_\mathrm{i}}{\omega} - k_\mathrm{d}\omega) \tag{19}$$

$$-C(\mathrm{j}\omega) = \frac{1}{G(\mathrm{j}\omega)} = \bar{G}(\mathrm{j}\omega) \tag{20}$$

From (17), (19) and (20), it follows that

$$-k_\mathrm{p} + \mathrm{j}(\frac{k_\mathrm{i}}{\omega} - k_\mathrm{d}\omega) = \frac{(\mathrm{j}\omega + T_1)(\mathrm{j}\omega + T_2)}{k}\mathrm{e}^{\mathrm{j}\tau\omega} \tag{21}$$

The real and imagery parts of left hand side and right hand side of (21) are equal, respectively.

$$\begin{aligned}&\mathrm{Re}[\bar{G}(\mathrm{j}\omega)] = \mathrm{Re}\left[\frac{(\mathrm{j}\omega + T_1)(\mathrm{j}\omega + T_2)}{k}\mathrm{e}^{\mathrm{j}\tau\omega}\right] = \\ &\frac{1}{k}[(T_1T_2 - \omega^2)\cos(\tau\omega) - (T_1 + T_2)\omega\sin(\tau\omega)] = \\ &\mathrm{Re}[-C(\mathrm{j}\omega)] = -k_\mathrm{p}\end{aligned} \tag{22}$$

$$\begin{aligned}&\mathrm{Im}[\bar{G}(\mathrm{j}\omega)] = \mathrm{Im}\left[\frac{(\mathrm{j}\omega + T_1)(\mathrm{j}\omega + T_2)}{k}\mathrm{e}^{\mathrm{j}\tau\omega}\right] = \\ &\frac{1}{k}[(T_1T_2 - \omega^2)\sin(\tau\omega) + (T_1 + T_2)\omega\cos(\tau\omega)] = \\ &\mathrm{Im}[-C(\mathrm{j}\omega)] = \frac{k_\mathrm{i}}{\omega} - k_\mathrm{d}\omega\end{aligned} \tag{23}$$

From Definitions 1 and 2, intersections of the INC and the NFCL are just real roots of $\delta_r(\omega_z)$. These intersections satisfy $\mathrm{Re}[\bar{G}(\mathrm{j}\omega)] = \mathrm{Re}[-C(\mathrm{j}\omega)]$. As non-negative real zeros of $\delta_r(\omega_z)$ are considered, we just need parts of the INC of $G(\mathrm{j}\omega)$ for $\omega \in [0, +\infty)$.

When $\delta(z)$ in (14) is stable, according to Lemma 4, $\delta_r(\omega_z)$ and $\delta_i(\omega_z)$ have exactly $4L+3$ real roots for $\omega_z \in [-2L\pi + \pi/4, 2L\pi + \pi/4]$, and these roots interlace. As $\omega_z = 0$ is a zero of $\delta_i(\omega_z)$, zeros of $\delta_r(\omega_z)$ and $\delta_i(\omega_z)$ interlace meanwhile $\omega_z = \tau\omega$, it follows that $\delta_r(\omega_z)$ has $M_0 = 2L+1$ real roots and $\delta_i(\omega_z)$ has $M_0 + 1$ real roots for $\omega \in [0, (2L\pi + \pi/4)/\tau]$. □

Theorem 2. Define the intersections in Theorem 1 as $\omega_1, \omega_2, \cdots, \omega_{M_0} (0 = \omega_0 < \omega_1 < \omega_2 < \cdots < \omega_{M_0})$. For the characteristic quasi-polynomial of the closed-loop AQM system to be stable, it is necessary and sufficient that (24) has feasible solution and $M_0 = 2L+1$.

$$\begin{cases} \mathrm{Im}[-C(\mathrm{j}\omega_0)] \geq \mathrm{Im}[\bar{G}(\mathrm{j}\omega_0)] \\ \mathrm{Im}[-C(\mathrm{j}\omega_1)] \leq \mathrm{Im}[\bar{G}(\mathrm{j}\omega_1)] \\ \qquad\vdots \\ \mathrm{Im}[-C(\mathrm{j}\omega_{M_0})] \leq \mathrm{Im}[\bar{G}(\mathrm{j}\omega_{M_0})] \end{cases} \tag{24}$$

Proof. That inequality (24) has feasible solution means that real roots of $\delta_r(\omega_z)$ and $\delta_i(\omega_z)$ interlace[15]. The number of zeros of $\delta_r(\omega_z)$ is $M_0 = 2L+1$, and $\omega_0 = 0$ is a zero of $\delta_i(\omega_z)$. So, $\delta_r(\omega_z)$ and $\delta_i(\omega_z)$ have $M_0+M_0+1 = 4L+3$ real roots for $\omega \in [0, (2L\pi + \pi/4)/\tau]$. According to Lemma 4, it is the sufficient condition for $\delta(z)$ in (14) to be stable.

When $\delta(z)$ in (14) is stable, according to Lemma 4, $\delta_r(\omega_z)$ and $\delta_i(\omega_z)$ have exactly $4L+3$ real roots and these roots interlace. From Theorem 1, we have $M_0 = 2L+1$. For these roots interlace, inequality (24) must have feasible solution. □

2.3 Graphical approach

In Theorem 1, boundaries of the INC are given by $\omega = 0$ and $\omega = (2L\pi + \pi/4)/\tau$ mathematically. We will convert them to key points in the complex plane.

Definition 3. Let $\omega = 0$ and $\omega = (2L\pi + \pi/4)/\tau$ in (22), respectively. The first kind of key points are defined as

$$k_{A1} = -\mathrm{Re}[\bar{G}(\mathrm{j}\omega)]|_{\omega=0} = -\frac{T_1 T_2}{k} \tag{25}$$

$$k_{A2} = -\mathrm{Re}[\bar{G}(\mathrm{j}\omega)]|_{\omega=(2L\pi+\frac{\pi}{4})/\tau} \tag{26}$$

Definition 4. For $\omega \in [0, (2L\pi + \pi/4)/\tau]$, let $\dfrac{\mathrm{dRe}[\bar{G}(\mathrm{j}\omega)]}{\mathrm{d}\omega}|_{\omega=\omega_i} = 0$ in (22). The second kind of key points are defined as

$$k_{Bi} = -\mathrm{Re}[\bar{G}(\mathrm{j}\omega)]|_{\omega=\omega_i}, \quad i = 1, 2, 3, \cdots \tag{27}$$

Remark 3. Using (27) to calculate k_{Bi} is a little complicated. Bi is in nature the inflexion of $\mathrm{Re}[\bar{G}(\mathrm{j}\omega)]$ with respect to ω in the complex plane. At the same time, $A1$ is the starting point, and $A2$ is the ending point of the INC of $G(\mathrm{j}\omega)$ for $\omega \in [0, (2L\pi + \pi/4)/\tau]$.

With the help of Definitions 3, 4 and Remark 3, we could describe Theorems 1 and 2 in a graphical approach as follows.

Corollary 1. In the complex plane, for $\omega \in [0, (2L\pi + \pi/4)/\tau]$, we plot the INC of AQM plant in (6) to find out the first and the second kinds of key points $\{k_{A1}, k_{A2}, k_{Bi}\}, i = 1, 2, 3, \cdots$. We plot the NFCL of PID controller in (7) to make sure that the INC and NFCL have exactly $M_0 = 2L+1$ intersections for any $k_\mathrm{p} \in [k_{\mathrm{p}1}, k_{\mathrm{p}2}]$, where $k_{\mathrm{p}1}$ and $k_{\mathrm{p}2}$ belong to the key points. For the characteristic quasi-polynomial of the closed-loop AQM system to be stable, it is necessary that k_p belongs to $[k_{\mathrm{p}1}, k_{\mathrm{p}2}]$. The region $[k_{\mathrm{p}1}, k_{\mathrm{p}2}]$ is defined as interested region of proportional gain.

Corollary 2. In the complex plane, for any k_p that belongs to interested region of proportional gain in Corollary 1, we plot lines $\mathrm{Im}[-C(\mathrm{j}\omega_i)] = \mathrm{Im}[\bar{G}(\mathrm{j}\omega_i)], i = 0, 1, \cdots, M_0$ in (23). We could find a region for $\{k_\mathrm{i}, k_\mathrm{d}\}$ that satisfies (24). For the characteristic quasi-polynomial of the closed-loop AQM system to be stable, it is necessary and sufficient that $\{k_\mathrm{p}, k_\mathrm{i}, k_\mathrm{d}\}$ locates in this region. This region is defined as stabilizing region of controller parameters.

3 Stabilizing boundaries

3.1 Stabilizing region of controller parameters

Take the network parameters $N = 60$, $C = 3\,750$ packets/s, and $R_0 = 0.25$ s. It follows from (6) that

$$G(s) = \frac{117187.5}{(s+0.512)(s+4)} \mathrm{e}^{-0.25s} \tag{28}$$

Let $x = \mathrm{Re}[\bar{G}(\mathrm{j}\omega)]$ in (22), $y = \mathrm{Im}[\bar{G}(\mathrm{j}\omega)]$ in (23). From Definition 1, we plot the INC of AQM plant (28) in Fig. 2. We find that the real roots of $\delta_r(\omega) = 0$ and $\delta_i(\omega) = 0$ alternate along the direction of increasing ω. Between every two zeros of $\delta_i(\omega)$, there exists exactly one zero of $\delta_r(\omega)$.

In order to analyze the stability of the characteristic quasi-polynomial of the closed-loop AQM system, we pay more attention to the part of the INC shown in Fig. 3, which is a zoomed-in version of Fig. 2 for $\omega \in [0, (2\pi + \pi/4)/\tau]$. We mark out the first kind of key points $A1$, $A2$ and the second kind of key points $B1$, $B2$, $B3$.

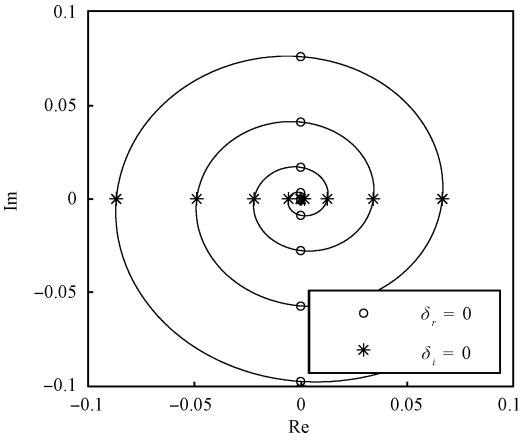

Fig. 2 The inverse Nyquist curve of the AQM system

In Fig. 3, from Definition 2, we find that if and only if the NFCL of PID controller locates between $A1$ and $B1$, there will be 3 intersections ($L = 1$). Two dashed lines denote $x = -k_{\mathrm{p}1} = 1.7476 \times 10^{-5}$ and $x = -k_{\mathrm{p}2} = -2.5501 \times 10^{-4}$, respectively.

From Corollary 1, the interested region of proportional gain is given by $k_\mathrm{p} \in [k_{\mathrm{p}1}, k_{\mathrm{p}2}]$. For the close-loop AQM system to be stable, it is necessary that proportional gain locates in this region.

From Corollary 2, for any $k_{\mathrm{p}0} \in (k_{\mathrm{p}1}, k_{\mathrm{p}2})$, we plot the NFCL of PID controller $x = -k_{\mathrm{p}0}$. There will be 3 inter-

sections, named as $\omega_1,\ \omega_2,\ \omega_3\,(0<\omega_1<\omega_2<\omega_3)$. From (23), for $i=0,1,2,3$, we plot lines

$$\frac{k_{\rm i}}{\omega_i}-k_{\rm d}\omega_i=\frac{1}{k}[(T_1T_2-\omega_i^2)\sin(\tau\omega_i)+(T_1+T_2)\omega_i\cos(\tau\omega_i)] \tag{29}$$

From (24), we have

$$\begin{aligned}
&\frac{k_{\rm i}}{\omega_0}-k_{\rm d}\omega_0\geq\frac{1}{k}[(T_1T_2-\omega_0^2)\sin(\tau\omega_0)+(T_1+T_2)\omega_0\cos(\tau\omega_0)]\\
&\frac{k_{\rm i}}{\omega_1}-k_{\rm d}\omega_1\leq\frac{1}{k}[(T_1T_2-\omega_1^2)\sin(\tau\omega_1)+(T_1+T_2)\omega_1\cos(\tau\omega_1)]\\
&\frac{k_{\rm i}}{\omega_2}-k_{\rm d}\omega_2\geq\frac{1}{k}[(T_1T_2-\omega_2^2)\sin(\tau\omega_2)+(T_1+T_2)\omega_2\cos(\tau\omega_2)]\\
&\frac{k_{\rm i}}{\omega_3}-k_{\rm d}\omega_3\leq\frac{1}{k}[(T_1T_2-\omega_3^2)\sin(\tau\omega_3)+(T_1+T_2)\omega_3\cos(\tau\omega_3)]
\end{aligned} \tag{30}$$

There exists a region for $\{k_{\rm i},k_{\rm d}\}$ satisfying (30), which is defined as the stabilizing region of $\{k_{\rm i},k_{\rm d}\}$.

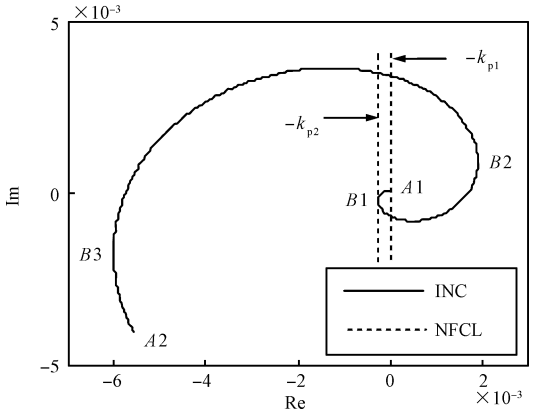

Fig. 3 Interested boundary of proportional gain

For $k_{\rm p0}=0.5\times10^{-4},1\times10^{-4},1.5\times10^{-4},2\times10^{-4}$, and 2.5×10^{-4}, respectively, using (29) and (30), we plot the stabilizing regions of $\{k_{\rm i},k_{\rm d}\}$ in Fig. 4. We conclude that with a fixed proportional gain, the stabilizing region of $\{k_{\rm i},k_{\rm d}\}$ is a triangle. Traversing over the proportional gain in interested region $[k_{\rm p1},k_{\rm p2}]$, we could confirm that the entire stabilizing region of $\{k_{\rm p},k_{\rm i},k_{\rm d}\}$ is a polyhedron, with cross section being triangle.

We can find out the traversing boundary of proportional gain based on Corollary 1. That is $k_{\rm p}\in[k_{\rm p1},k_{\rm p2}]$ in Fig. 3. Compared to those methods whose traversing boundary is given by empiricism in large scope, the proposed approach consumes lower complexity of calculation procedure to obtain the stabilizing region of $\{k_{\rm p},k_{\rm i},k_{\rm d}\}$.

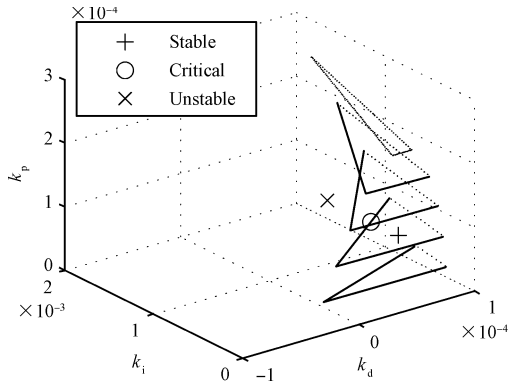

Fig. 4 Stabilizing region of controller parameters

3.2 Stabilizing boundary′s relations with network parameters

In the following, we turn our attention to analyzing the relations between stabilizing boundary of the proportional gain in PID controller and the network parameters.

Take network parameters $C=3\,750$ packets/s and $R_0=0.25$ s. N ranges from 40 to 300. For different N, we plot the INC, and mark out two kinds of key points. Then, we plot lines in (29) and check the stabilizing boundary of proportional gain by (30). Using the stability criterion given in previous sections, we confirm that the region below the curve $k_{\rm pmax}$ corresponds to the stabilizing region of $k_{\rm p}$ shown in Fig. 5 (a), and we find that the stabilizing boundary of $k_{\rm pmax}$ increases approximately linearly with N.

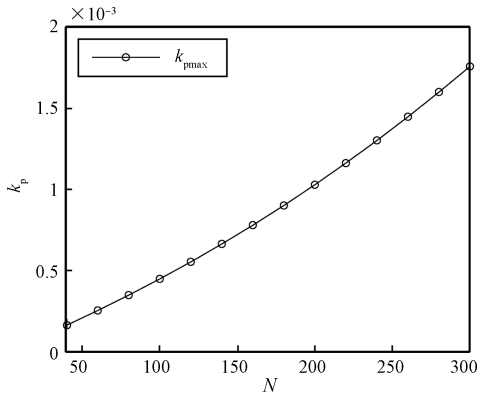

(a) Stabilizing region of $k_{\rm p}$ for different N

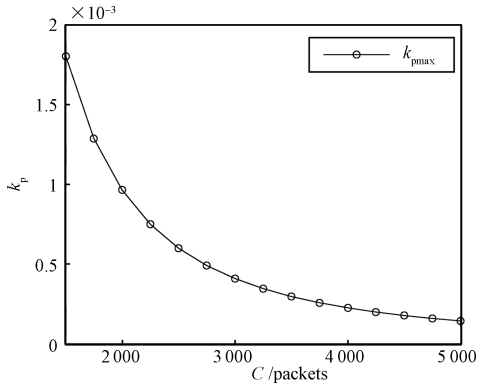

(b) Stabilizing region of $k_{\rm p}$ for different C

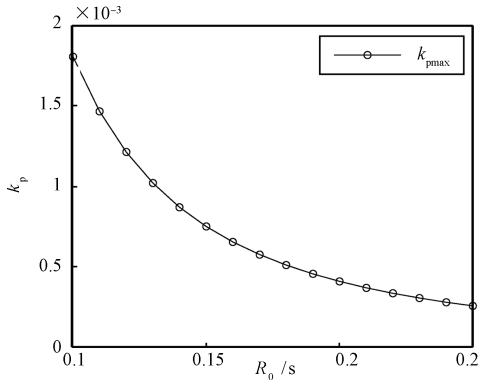

(c) Stabilizing region of $k_{\rm p}$ for different R_0

Fig. 5 Stabilizing regions of $k_{\rm p}$ for different network parameters (The stabilizing region is below the curve.)

In the same way, $N = 60$ and $R_0 = 0.25$ s. C ranges from 1 500 to 5 000 packets/s. The stabilizing region of $k_{\rm p}$ is shown in Fig. 5 (b). Then, $N = 60, C = 3\,750$ packets/s, R_0 ranges from 0.1 to 0.25 s. The corresponding stabilizing region of $k_{\rm p}$ is shown in Fig. 5 (c). From these two curves, we find that stabilizing boundary of $k_{\rm pmax}$ decreases approximately in inverse proportion with C and R_0, respectively.

3.3 Stabilizing boundary comparison

Result comparisons between ours and the ones in [13, 16] were conducted. Reference [13] discussed stabilizing proportional gain of the PI controller by Jacobi matrix in parameter space. Reference [16] gave the delay-dependent stability criterion using the Lyapunov sufficient condition. The proportional gain regions are estimated in Table 1, as functions of round-trip time delay.

From Table 1, we find that the smallest proportional gain region is given by [16] based on Lyapunov criterion, which is a sufficient condition for system to be stable. Although [13] gives a necessary and sufficient condition based on parameter space, the result is conservative for its controller is of PI type $C(s) = k_{\rm pi}(1 + \frac{1}{T_{\rm i}s})$, which gives the stabilizing boundary of $k_{\rm pi}$ with a fixed integral time constant $T_{\rm i}$ in two-dimensional plane.

It is clear that our result is less conservative than those in [13, 16]. Two reasons explain its superiority: 1) Our approach is based on a necessary and sufficient condition; 2) Our controller is of PID type $C(s) = k_{\rm p} + k_{\rm i}/s + k_{\rm d}s$, which gives the stabilizing boundary of $k_{\rm p}, k_{\rm i}$ and $k_{\rm d}$ in three-dimensional space. As derivative element is adopted, stabilizing region of proportional gain for close-loop AQM system stable is extended.

Table 1 Comparison of stabilizing proportional gains between the results in [13, 16] and the proposed approach

R_0(s)($\times 10^{-4}$)	0.20	0.25	0.30	0.35
In [16]	2.6314	1.5920	1.0546	0.7425
In [13]	2.7176	1.6412	1.0857	1.0857
Proposed	4.0690	2.5501	1.7462	1.2701

4 Simulation

4.1 Simulation in Matlab

To verify the stabilizing region, we conducted simulations by Matlab. The AQM plant and network parameters are given in (28). The controller is of PID type with parameters $\{k_{\rm p}, k_{\rm i}, k_{\rm d}\}$.

In Fig. 4, setting $k_{\rm p0} = 1 \times 10^{-4}$, we obtain the stabilizing region of $\{k_{\rm i}, k_{\rm d}\}$ in a triangle graph. Setting $k_{\rm d0} = 0.5 \times 10^{-4}$, we obtain the stabilizing boundary of $k_{\rm i}$, $k_{\rm i} \in [0, 5.1 \times 10^{-4}]$. Let $k_{\rm i0} = 2 \times 10^{-4}, k_{\rm i1} = 5.1 \times 10^{-4}$, and $k_{\rm i2} = 10 \times 10^{-4}$. We obtain three groups of controller parameters. $\{k_{\rm p0}, k_{\rm i0}, k_{\rm d0}\}$ locates inside the stabilizing region, $\{k_{\rm p0}, k_{\rm i1}, k_{\rm d0}\}$ locates on the stabilizing boundary, and $\{k_{\rm p0}, k_{\rm i2}, k_{\rm d0}\}$ locates outside the stabilizing region.

With these three groups of controller parameters, we picture the step responses of δq in Fig. 6, respectively. We find that $\{k_{\rm p0}, k_{\rm i0}, k_{\rm d0}\}$ controls the output convergence, $\{k_{\rm p0}, k_{\rm i1}, k_{\rm d0}\}$ controls the output flapping, and $\{k_{\rm p0}, k_{\rm i2}, k_{\rm d0}\}$ controls the output flapping divergence. The result has validated our analysis.

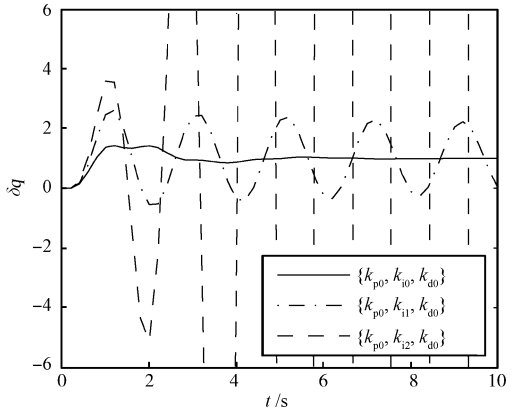

Fig. 6 Step responses of δq for different PID parameters

4.2 Simulation in NS

To verify the stabilizing region in network environment, we conducted nonlinear simulations by NS, using the network topology depicted in Fig. 7.

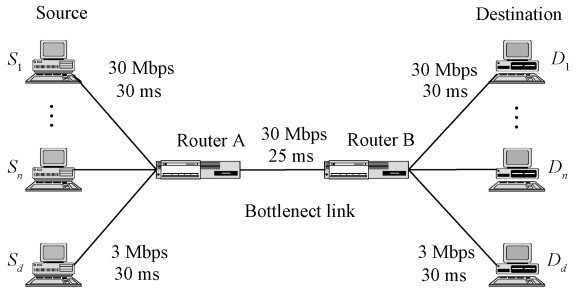

Fig. 7 Simulation network topology

$S_i\,(i = 1, \cdots, n)$ are TCP senders with average packet size being 1 000 Bytes. S_d is a UDP sender which has 3 Mbps capacity and 30 ms propagation delay, generating the realistic traffic scenarios. The only bottleneck link lies between Router A and Router B, which has 30 Mbps capacity and 25 ms propagation delay. Other links have 30 Mbps capacity and 30 ms propagation delay. Router A uses the PID controller to implement active queue management, others use the Drop Tail. The sampling frequency is 160 Hz. The buffer size is 1 125 packets and the desired queue length is 300 packets, giving 80 ms queuing delay. Together with the propagation delay of 170 ms, the round-trip time delay is about 250 ms. The simulation lasted for 200 s, and the UDP started sending packets as CBR disturbance at time $t = 100$ s.

Experiment results are illustrated in Figs. 8 and 9. As one of the controller parameters inside the stabilizing region, $\{k_{\rm p0}, k_{\rm i0}, k_{\rm d0}\}$ regulates the queue length to the desired 300 packets pictured in Fig. 8 (a). Fig. 8 (b) shows a little oscillation in the case of controller parameters $\{k_{\rm p0}, k_{\rm i1}, k_{\rm d0}\}$ on the stabilizing boundary, when it is critically stable. Fig. 8 (c) shows significant oscillation in the case of $\{k_{\rm p0}, k_{\rm i2}, k_{\rm d0}\}$ outside the region, when it is unstable.

Fig. 9 shows the drop probabilities corresponding to the above conditions. When it is stable, the drop probability remains around 0.005, as shown in Fig. 9 (a). When it is critically stable, the drop probability fluctuates under 0.01, as shown in Fig. 9 (b). When it is unstable, the drop probability oscillates between 0 and 0.02 significantly, as

shown in Fig. 9 (c).

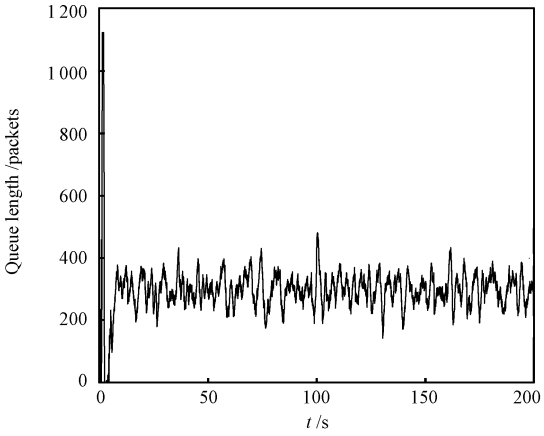

(a) $\{k_{\rm p0}, k_{\rm i0}, k_{\rm d0}\}$ inside the stabilizing region

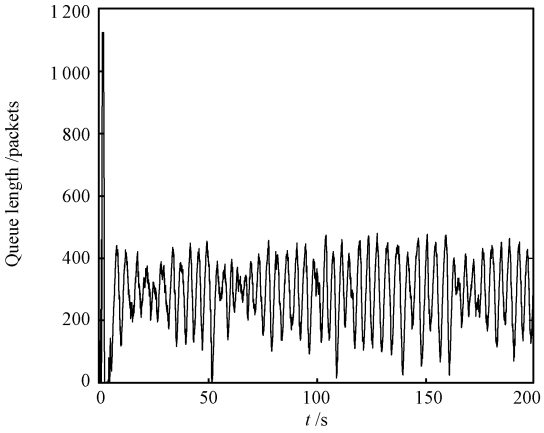

(b) $\{k_{\rm p0}, k_{\rm i1}, k_{\rm d0}\}$ on the stabilizing boundary

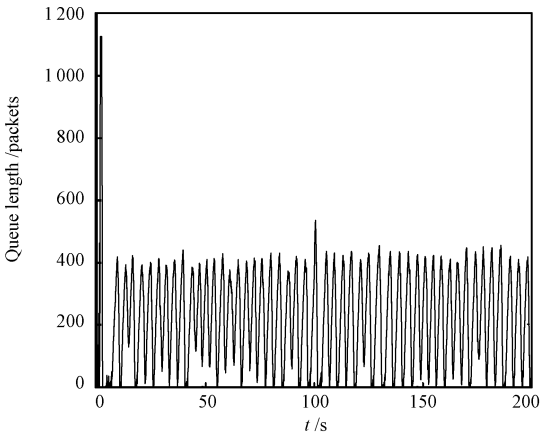

(c) $\{k_{\rm p0}, k_{\rm i2}, k_{\rm d0}\}$ outside the stabilizing region

Fig. 8 Instantaneous queue lengths for different PID parameters

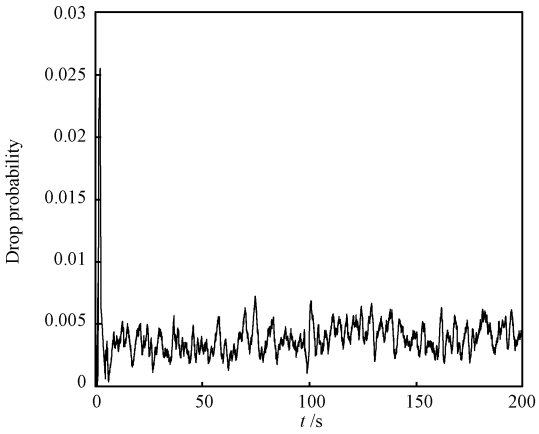

(a) $\{k_{\rm p0}, k_{\rm i0}, k_{\rm d0}\}$ inside the stabilizing region

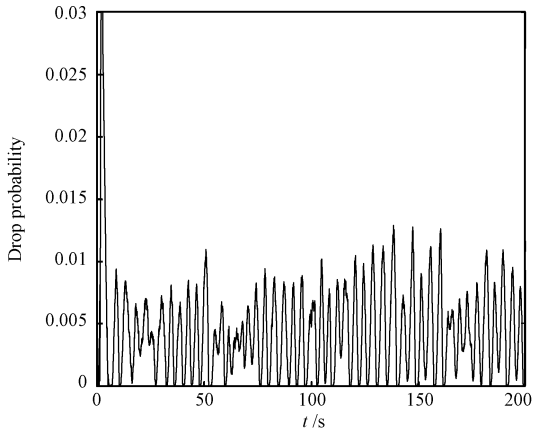

(b) $\{k_{\rm p0}, k_{\rm i1}, k_{\rm d0}\}$ on the stabilizing boundary

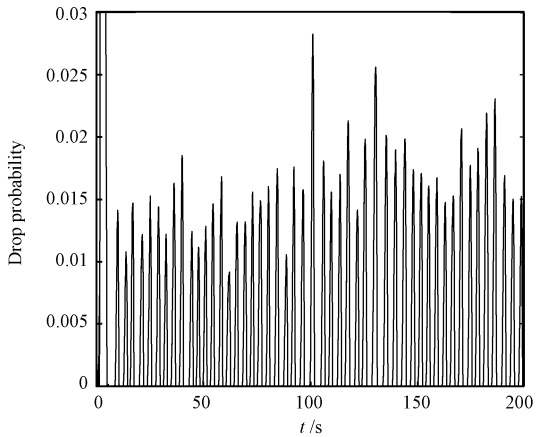

(c) $\{k_{\rm p0}, k_{\rm i2}, k_{\rm d0}\}$ outside the stabilizing region

Fig. 9 Instantaneous drop probabilities for different PID parameters

5 Conclusion

This paper discusses the stability characteristic of TCP/AQM networks using the PID controller. It is based on the necessary and sufficient stability criterion developed in complex plane. The stabilizing region of AQM controller in PID type is given. The relations between stabilizing boundary of proportional gain and network parameters are illuminated. Simulation experiments conducted by Matlab and NS have validated our criterion. Comparison results show that our approach is less conservative than the previous ones. Excellence of the proposed method lies in the lower complexity of the calculation procedure and intuition in the complex plane. In this paper, we have just considered a simplified version of TCP/AQM model for facility. For a complete model, we will carry on the research in our future work.

References

1 Floyd S, Jacobson V. Random early detection gateways for congestion avoidance. *IEEE/ACM Transactions on Networking*, 1993, **1**(4): 397−413

2 Misra V, Gong W B, Towsley D. Fluid-based analysis of a network of AQM routers supporting TCP flows with an application to RED. *ACM SIGCOMM Computer Communication Review*, 2000, **30**(4): 151−160

3 Hollot C V, Misra V, Towsley D, Gong W B. Analysis and design of controllers for AQM routers supporting TCP flows. *IEEE Transactions on Automatic Control*, 2002, **47**(6): 945−959

4 Ren F Y, Lin C, Wei B. A nonlinear control theoretic analysis to TCP-RED system. *Computer Networks*, 2005, **49**(4): 580−592

5 Sun J S, Zukerman M, Palaniswami M. A stable adaptive PI controller for AQM. In: Proceedings of International Symposium on Communications and Information Technologies. Sydney, Australia: IEEE, 2007. 707−712

6 Jing Yuan-Wei, Zeng Hui, Pan Wei. Pole assignment algorithm in networks traffic control. *Control and Decision*, 2006, **21**(5): 492−496 (in Chinese)

7 Kim K B. Design of feedback controls supporting TCP based on the state-space approach. *IEEE Transactions on Automatic Control*, 2006, **51**(7): 1086−1099

8 Yang Ji-Wen, Gu Dan-Ying, Zhang Wei-Dong. An analytical design method of PID controller based on AQM/ARQ. *Journal of Software*, 2006, **17**(9): 1989−1995 (in Chinese)

9 Zheng F, Nelson J. An H_∞ approach to the controller design of AQM routers supporting TCP flows. *Automatica*, 2009, **45**(3): 757−763

10 Wang Xiu-Li, Wang Yong-Ji, Zhou Hui, Cai Kai-Yuan. Optimal design of AQM routers with D-stable regions based on ITAE performance. *Journal of Software*, 2007, **18**(12): 3092−3103 (in Chinese)

11 Chen C K, Kuo H H, Yan J J, Liao T L. GA-based PID active queue management control design for a class of TCP communication networks. *Expert Systems with Applications*, 2009, **36**(2): 1903−1913

12 Hollot C V, Chait Y. Nonlinear stability analysis for a class of TCP/AQM networks. In: Proceedings of the 40th IEEE Conference on Decision and Control. Orlando, USA: IEEE, 2001. 2309−2314

13 Wang De-Jin. Stability analysis of PI TCP/AQM networks: a parameter space approach. *Acta Automatica Sinica*, 2007, **33**(7): 756−760

14 Oliveira V A, Teixeira M C M, Cossi L. Stabilizing a class of time delay systems using the Hermite-Biehler theorem. *Linear Algebra and Its Applications*, 2003, **369**(1): 203−216

15 Silva G J, Datta A, Bhattacharyya S P. New results on the synthesis of PID controllers. *IEEE Transactions on Automatic Control*, 2002, **47**(2): 241−252

16 Wu M, He Y, She J H. New delay-dependent stability criteria and stabilizing method for neutral systems. *IEEE Transactions on Automatic Control*, 2004, **49**(12): 2266−2271

GE Long Ph. D. candidate at the School of Automation, Nanjing University of Science and Technology. He received his bachelor and master degrees from Nanjing University of Science and Technology in 2004 and 2006, respectively. His research interest covers analysis and control of complex networked systems and intelligent information processing. Corresponding author of this paper.
E-mail: gelong@mail.njust.edu.cn

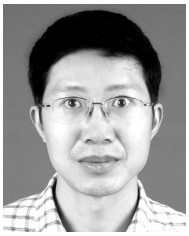

FANG Bin Professor at Nanjing University of Science and Technology. His research interest covers control theory and application.
E-mail: fangbin@mail.njust.edu.cn

SUN Jin-Sheng Professor at Nanjing University of Science and Technology. His research interest covers congestion control and fault-tolerant control.
E-mail: jssun67@yahoo.com.cn

WANG Zhi-Quan Professor at Nanjing University of Science and Technology. His research interest covers fault-tolerant control and networked control systems.
E-mail: wangzqwhz@yahoo.com.cn